RESERVOIR IMAGING OF THE SIBAYAK GEOTHERMAL FIELD, INDONESIA USING BOREHOLE-TO-SURFACE RESISTIVITY MEASUREMENTS

YUNUS DAUD[1], JATMIKO PRIO ATMOJO[2], SAYOGI SUDARMAN[3] & KEISUKE USHIJIMA[1]

[1]Exploration Geophysics Lab., Graduate School of Engineering, Kyushu University, Fukuoka, Japan
[2]Energy Resources Eng. Lab., Graduate School of Engineering, Kyushu University, Fukuoka, Japan
[3]Geothermal Division, Pertamina, Jakarta, Indonesia

SUMMARY - Borehole-to-surface resistivity (Mise-a-La-Masse) measurements were carried out in the Sibayak Geothermal Field in November 1995 using the exploration well **SBY-1** and the production well **SBY-4.** The object of this survey is to image a promising reservoir zone and to correlate the results with formation temperatures and lost circulation zones. The results will be used to plan future development of the Sibayak geothermal field. In this *study,* the formation temperature and lost circulation zone data fkom the existing wells are also presented as a comparison to the Mise-a-La-Masse data interpretation. This Mise-a-La-Masse data interpretation indicates that the reservoir zone trends to the north - northeast of the *study* area and shows good correlation with formation temperature and lost circulation zone. The most prospective target surrounds well SBY-5 which is the best target for future development. This study has shown that the Mise-a-La-Masse method *can* be used to image a geothermal reservoir.

1. INTRODUCTION

The Mise-A-La-Masse (MAM) technique is a geophysical tool for quickly mapping the low resistivity area encountered in the highly fractured reservoir zones (Kauahikaua, et.al., 1980, Tagomori et.al., 1984, Ushijima, 1989). The Mise-a-La-Masse method was first developed and used by C. Schlumberger in 1920 for mineral exploration The method utilizes a buried current electrode (point source of current) within a conductive body of interest., and the other current electrode is placed at *great* distance away fkom the anomalous mass. The method involves borehole-to-surface measurements and is one of the modern electrical tomography methods (Ushijima et al., 1990). However, the borehole-to-surface method utilizing a buried current electrode (point source of current) has some limitations when applied to geothermal exploration because of the high temperatures of wells. Therefore, a casing pipe *can* be used as a line source of current instead of a buried point source of current. According to Tagomori et al. (1984), for a geothermal reservoir that is electrically charged by the casing pipe, the shape of the potential lines directly reflects the geometry of the reservoir. Geothermal fluid has low resistivity, so that the geothermal reservoir itself *can* be considered as a subsurface conductor similar to an ore body.

In order to image the shape of the reservoir and correlate temperature and lost circulation zones, the MAM survey was carried out using the exploratory well **SBY-1** and the production well **SBY-4.** The anchor casings of **SBY-1** and **SBY-4** were selected as current electrodes C1 because the well locations enabled maximum coverage. Well **SBY-1** is almost vertical with a total depth of 1501 m (1495 m vertical depth), whereas well **SBY-4** is a directional well with a total depth 2181 m (or 1879 m vertical depth), which was cased to 2172 m.

Figure 1. Location Map of Sibayak Geothermal Field, Indonesia

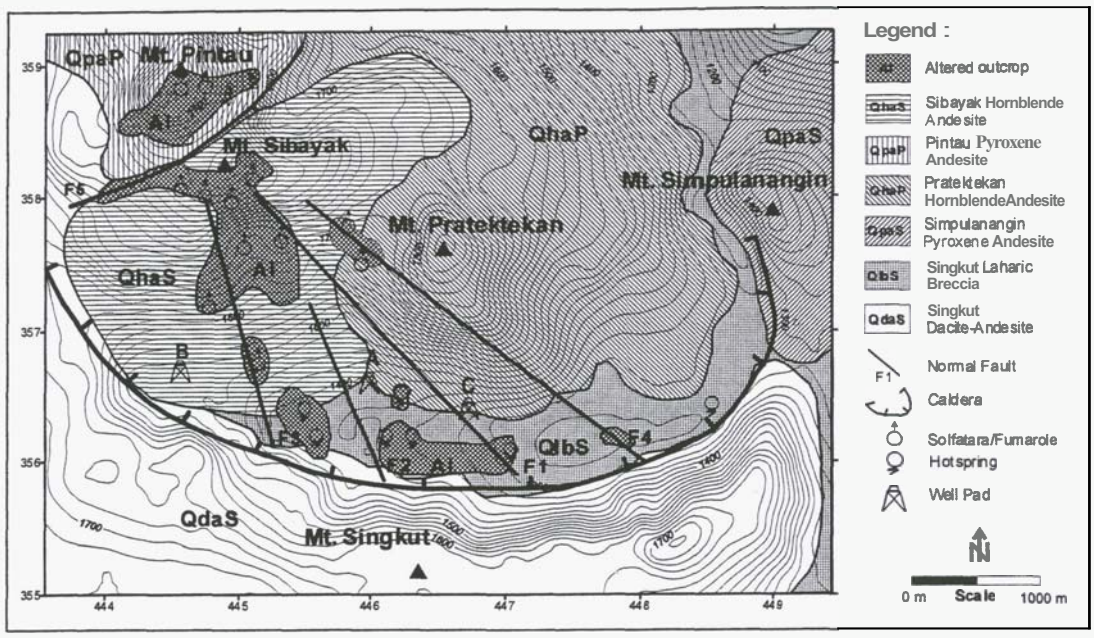

Figure 2. Geological Map of Sibayak Geothermal Field

2. GEOLOGICAL SETTING AND SURFACE MANIFESTATIONS

Sibayak Geothermal Field is located at about 65 km to the southwest of Medan in the North Sumatera Province, Indonesia (Fig. 1). It is situated in a **high** relief area inside the large Singkut caldera.

The Sibayak area is composed of pre-Tertiary to Tertiary sedimentary formations in the lower part that are unconformably overlain by Quaternary volcanic formation. The sedimentary formation is predominantly sandstone followed by shale and limestone. In the **area** of the Singkut caldera, the Quaternary volcanic rock formation is divided into pre and post caldera units. The former includes Singkut &cite-andesite and Singkut laharic breccia, and the latter includes Simpulanangin pyroxene andesite, Pratetekan hornblende andesite, Pintau pyroxene andesite and Sibayak hornblende andesite (Fig. **2).**

Drilling data show that the sedimentary formation is generally found 1150m below the surface. The sedimentary formation was intensively hydrothexmally altered. This formation is **mainly** composed of sandstone with intercalated shale **and** sporadic limestone. The volcanic rock formation is composed of andesite, andesite breccia and tuff breccia. Relatively moderate clay and chloritic hydrothermal alteration are found within this formation. Intense hydrothermal alteration **of** silicification and argilization occur within the sedimentary formation.

The geological structure in the Sibayak area is mainly controlled by volcanic and tectonic processes. The caldera structure is elongated NW-SE, and it developed after the Mt. Singkut volcanic eruption. Some fault structures within the caldera are oriented **NW-SE** and extend to the center of Mt. Sibayak - Mt. **Pintau,** where they are cross cut by **NE-SW** fault structures (F5) (Fig. **2).** The fault structures within the caldera are associated with down dropped block **as** indicated **by** the surface topography. Intense fracture controlled permeability **is** inferred fi-om shallow to deep circulation losses during **drilling.**

3. THEORETICAL BACKGROUND

The potential due to **a** point-source electrode at a distance r is

$$V = \frac{\rho I}{2\pi} \frac{1}{r} \qquad (1)$$

if the potential at **an** infinite distance is assumed to be zero.

The potential of a line source electrode is described by Kauahikaua et al. (1980). The formula can be derived by a process of integration **starting fiom** the potential of a point electrode:

$$V = \frac{\rho I}{2\pi} \frac{1}{\lambda} \ln \frac{\lambda + \sqrt{\lambda^2 + r^2}}{r} \qquad (2)$$

Therefore, the expression for the apparent resistivity for the **four** electrodes configuration shown in Figure **3** is expressed **as:**

$$\rho_a = K \frac{V}{I} \qquad (3)$$

where K is called a geometric factor and defined by the following equation:

$$K = 2\pi \left\{ \frac{1}{\lambda} \ln \frac{P_2C_1(\lambda + \sqrt{\lambda^2 + (P_1C_1)^2})}{P_1C_1(\lambda + \sqrt{\lambda^2 + (P_2C_1)^2})} - \frac{1}{P_1C_2} + \frac{1}{P_2C_2} \right\}^{-1} \qquad (4)$$

Topographic effects and deflection of the casing pipe for the directional drilling should be

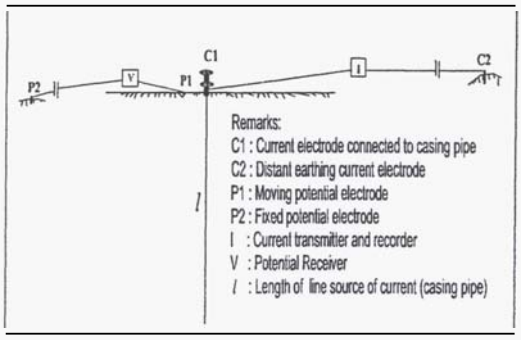

Figure 3. Field Layout of the Mise-a-La-Masse Measurements.

considered for the geometric factor. The equipotential surfaces approach a spherical form in the neighborhood of the current electrode when the subsurface is isotropic and homogeneous formations.

4. FIELD MEASUREMENTS

Mise-a-La-Masse measurements were carried out by injecting a current through current electrodes (C_1) connected to the anchor casing of wells SBY-1 and SBY-4, respectively (Fig. 3). The total depth of wells SBY-1 and SBY-4 are 1501 m (or 1495 m true vertical depth) and 2181 m (or 1879 m true vertical depth), respectively. While the azimuth of wells SBY-1 and SBY-4 is N 87° W and N 70" E, respectively. The distant earthing C_2 is 4.5 km fiom the well SBY-1. The potential difference was measured through potential electrodes P_1 and P_2. The potential electrode P_1 was moved radially fiom the C_1 electrode with 100 m separation. The potential electrode P_2 was set far away fiom the wellhead (C_1). The position of potential electrode P_2 was chosen specifically in a position which is noise free fiom electric and magnetic fields. The potential electrode P_2 for the current electrode (C_1) of well SBY-1 was placed in the northeastern part of the surveyed area about 2.5 km away fiom SBY-1. For the current electrode (C_1) of the well SBY-4, the potential electrode P_2 was located in the northwestern part of the surveyed area 2.5 km away fiom the well SBY-4. Potential measurements were also conducted using a fixed potential electrode P_1' located about 50 m away fkom the charged well (C_1), in order to confirm a stable potential measurement.

The main geoelectrical equipment used in this survey was a transmitter (Geosource type P3FT-LIPI) with 6 A output, supported by 5 kVA power supply (Yanmar generator), and a receiver (Fluke-87/USA), with a sensitivity of 0.01 mV. The potential electrodes P1 and P2 were immersed with saturated copper sulfate solution in porous pots, in order to eliminate the polarization effects during measurements.

At Sibayak MAM measurements were conducted along 14 survey lines (163 points) around SBY-1. Near SBY-4, the measurements were conducted along 12 survey lines (148 points). The survey lines could not be made over the same length due to field conditions.

5. MISE-A-LA-MASSE DATA PROCESSING *AND* INTERPRETATION

The actual potential difference V measured at each station was transformed into apparent resistivity using Equation (3). The apparent resistivity value represents the total response of subsurface conditions. In order to recognize the response of any anomalous body, the apparent resistivity value is subtracted fiom the theoretical apparent resistivity value to get the residual apparent resistivity anomaly.

The apparent resistivity values measured using SBY-1 (Fig. 4) indicate a low resistivity zone (less than 10 ohm-m) to the northwest. This low resistivity anomaly is probably due to subsurface thermal activity in the area. The apparent resistivity values increase to the east and southeast fiom SBY-1 probably due to decrease in subsurface thermal activity. The orientation of the contour pattern trending to the northwest is thought to be influenced by fault structures (see also Fig. 2).

The MAM results from SBY-4 (Fig. 5) show a low resistivity zone (less than 10 ohm-m) to the north and northeast fiom the well covering the same area as interpreted fiom the well SBY-1. Furthermore, the lowest apparent resistivity anomaly (less than 8 ohm-m) is encountered around well SBY-5. The apparent resistivity values increase gradually to the southwest and southeast. This is thought to be caused by the decrease in subsurface thermal activity.

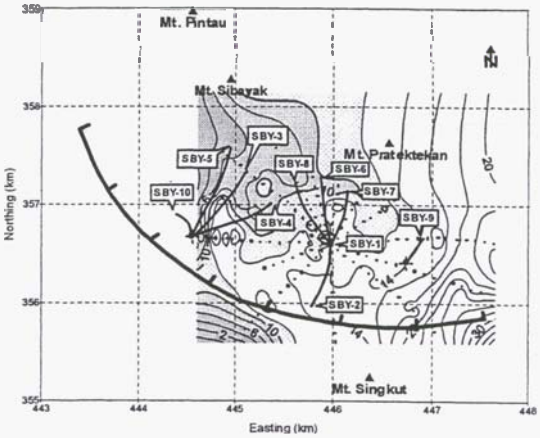

Figure 4. Apparent Resistivity Map fiom Well SBY-1 of the Sibayak Geothennal Field. Values in the contours are in Ohm-m.

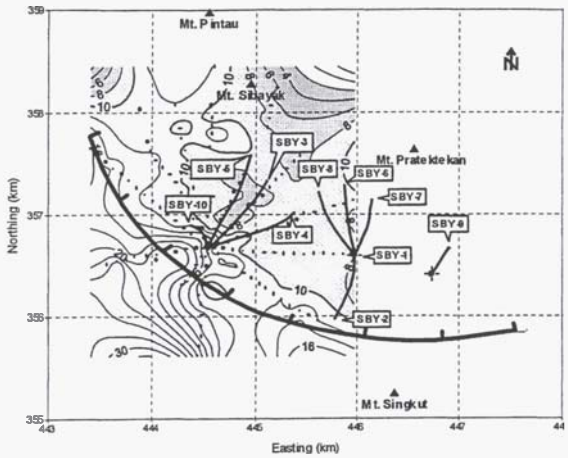

Figure 5. Apparent Resistivity Map from Well SBY-4 of the Sibayak Geothermal Field. The values in the contours are in Ohm-m.

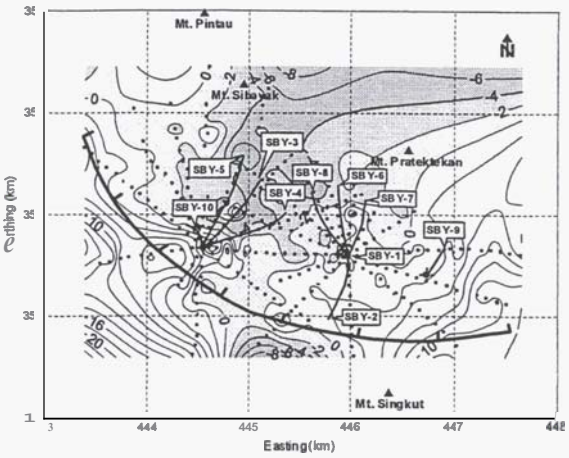

Figure 6. Apparent Resistivity **Map** from Wells SBY-1 **and** SBY-4 **of** the Sibayak Geothermal Field. The contour values are in Ohm-meter.

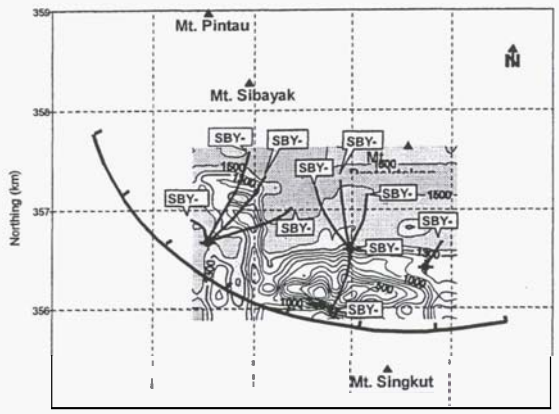

Figure 7. Distribution of lost circulation zones of the Sibayak Geothermal Field The contour values are in kg/hr

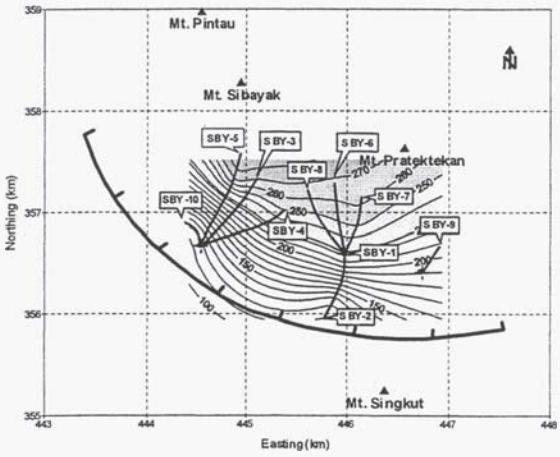

Figure 8. Formation temperature distribution in -500 m depth of the Sibayak Geothermal Field. The values in the contours are in ^{0}C.

Tabel 1. Wellbore Data **of** Sibayak Geothermal Field **(status** September 1998)

No	Data	Dimension	SBY-I	SBY-2	SBY-3	SBY-4	SBY-5	SBY-6	SBY-7	SBY-8	SBY-9	SBY-10
1	Type		Exploration	Exploration	Exploration	Development	Development	Development	Development	Development	Development	Development
2	Elevation	m a.s.l.	1384	1384	1468	1468	1384	1384	1384	1384	1337	1468
3	Total depth	MvD	1498	2116	1880	1880	1994	1750	2096	1935	1527	2164
4	Temp. at Total Depth	°C	243	104	272	274	284	251	227	260	220	140
5	Max.Temp. in Depth	°C MmD	243 1320	104 1650	272 1780	274 1610	302 2025	270 1475	266 1600	270 1800	236 1350	170 400
6	Production: Steam+Water	ton/hr	72		95	156	216	197		158		
7	Output	MWe	2		3	3	6	4		3		

In order to get clearer imaging of the anomalous body, the residual apparent resistivity anomaly is calculated fiom the apparent resistivity data measured using the wells SBY-1 and SBY-4. The results are then combined and presented in one map (Fig. *6).* The combined map shows that the main distribution of the residual apparent resistivity anomaly is similar to the distribution of the resistivity anomaly. Figure 6 also shows that the negative residual anomaly extends northeast fiom well SBY-4 and northwest from well SBY-1 reflecting the position of the reservoir. The southwestern boundary of the Singkut caldera is clearly reflected by the contrast between the negative anomaly (inside the caldera) and the positive anomaly (outside the caldera). The other interesting negative residual anomaly occurs just outside the southern caldera rim.

6. DISTRIBUTION OF FORMATION TEMPERATURES AND LOST CIRCULATION ZONES

By 1997, ten exploration wells were drilled at the Sibayak Geothermal Field. The reservoir is mainly controlled by geological structures (fracture zones). The locations of the fracture zones were identified by the occurrence of lost circulation zones encountered during well completion. High or total lost circulation zones were found in all of the existing wells at variable depths, whereas feed zones were also recognized from the formation temperature and pressure data. The distribution of lost circulation zones at depth -450 m a.s.l. are shown in Figure 7. They occur in the north and northeast part of the study area as well as in the southern part outside the Singkut caldera rim. Lost circulation zones also occur near Mt. Pratektekan as indicated by the wells SBY-7 and SBY-9 data.

The formation temperatures in the Sibayak geothermal field were measured in the existing wells during well-completion tests. The formation temperature distribution at -500 m depth is shown in Figure 8. The distribution of high temperatures (more than 250 °C) occurs to the north, beneath Mt. Sibayak and to the northeast beneath Mt. Pratektekan. The highest temperature zone (about 280 "C) was observed beneath the eastern flank of Mt. Sibayak near to the largest fumarole in the area.

The production well data of the Sibayak Geothermal Field as well as the formation temperature data are summarized in the Table 1. The most productive well is SBY-5, whose total production is 57 ton/hr steam, which is equivalent to 6 Mwe.

7. DISCUSSION

The results of MAM survey and other related well-bore data are presented in Figure 9. The most interesting feature is a negative residual resistivity zone centered to the northeast from well SBY-4 and to the northwest fiom well SBY-1. This zone includes the known high temperature production zone and high lost circulation zone. Almost all of the production wells (i.e., wells SBY-3, 4, 5, 6, 7 and 8) are located within the negative residual resistivity zone.

Furthermore, the most productive well (i.e. well SBY-5) is located inside the lowest residual resistivity zone (-6 Ohm-m) close to the eastern flank of Mt. Sibayak. The negative residual resistivity zone correlates with high formation temperatures and high permeabilities. The negative residual resistivity zone tends to extend in a north - northeast direction and could be the best target for further exploration.

Another negative residual resistivity anomaly is found in the southem part outside the southern caldera rim. This anomaly correlates with a high lost circulation zone in the same location, but the temperature is low as indicated by the well SBY-2. This anomaly might be caused by a permeable formation filled by cold water inflowing towards the main reservoir (natural recharge).

The geometry of the anomalous body indicated by the MAM data can be assessed by three-dimensional modelling; software development for this is in progress.

8. CONCLUSIONS

This MAM data reveals the reservoir zone in the Sibayak geothermal field to the northeast and includes the known geothermal reservoir. The anomaly correlates with formation temperatures and lost circulation zones. The most prospective zone for future exploration is in the vicinity of SBY-5.

9. ACKNOWLEDGMENTS

The authors wish to express their gratitude to the Management of Pertamina for their permission to publish this paper. The first author (Yunus Daud) gratefully acknowledges support fiom a postgraduate scholarship awarded by the Hitachi Scholarship Foundation, Tokyo, Japan.

10. REFERENCES

Gunderson, R.P., Dobson P.F., Sharp W.D., Pujianto R. and Hasibuan A. (1995). Geology and thermal features of the Sarulla contract area, north Sumatra, Indonesia, *Proceeding of the World Geothermal Congress,* Florence, Italy 10-31 May, pp.687-692.

Kauahikaua, J., Mattice, M. and Jackson, D. (1980). Mise-8-la-masse mapping of the HGP-A geothermal reservoir, Hawai, ***Geothermal Resources Council Trans.,*** Vol. 4, pp.65-68.

Tagomori, K., Ushijima, K. and Kinoshita, Y. (1984). Direct detection of geothermal reservoir at Hatchobaru geothermal field by the Mise-á-la-masse measurements, ***Geothermal Resources Council Trans.,*** Vol. *8,* pp.5 13-516.

Ushijima, K. (1989). Exploration of geothermal reservoir by the Mise-Cla-masse measurements, ***Geothermal Resources Council Bull.,*** Vol. 18 (2), pp. 17-25.

Ushijima, K., Mizunaga, H., and Kaieda, H. (1990). Fluid Flow Monitoring Using Electrical Prospecting, ***The First SEGJ/SEG International Symposium on Geotomography,*** Vol.1, pp. 271-279.

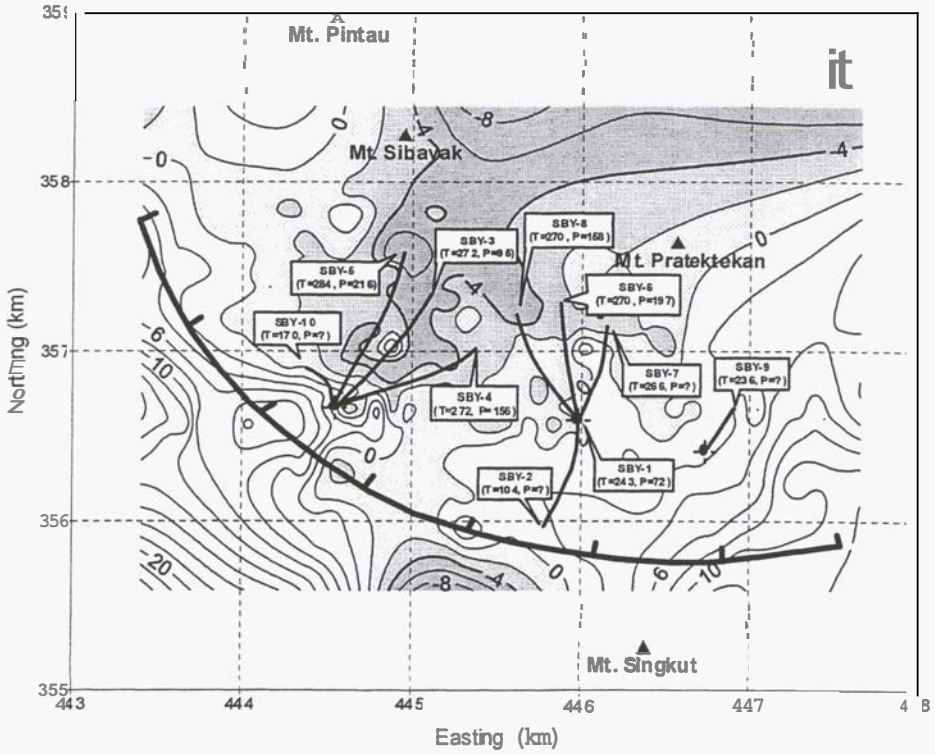

Figure *9.* Distribution of negative residual apparent resistivity of MAM data and related well-bore data of the Sibayak Geothermal Field. (T = down-hole temperature in °C and P = well production in ton/hr).